Phosphorus Catalysis Enabling α-sp^3-C–H Amination of 2-Alkylpyridines

Received 00th January 20xx,
Accepted 00th January 20xx

DOI: 10.1039/x0xx00000x

Yoshito Heike,[a] Asa Tagata,[a] Akira Yada,[b,c] Kanako Nozawa-Kumada,[b] Masaya Sawamura,*[a,d] and Yohei Shimizu*[a,d,e]

Phosphorus-catalyzed sp^3-C–H amination of 2-alkylpyridines was developed as a notable advancement of a catalytic sp^3-C–H functionalization by an organophosphorus compound. Racemic 2,2'-bis(diphenylphosphino)-1,1'-binaphthyl (BINAP) acted as a particularly efficient catalyst precursor for the reaction of 2-alkylpyridines with dibutyl azodicarboxylate (DBAD) as an aminating agent in the presence of water and cesium carbonate as promoters in dichloromethane as a critical solvent, allowing the sp^3-C–H amination under mild reaction conditions at 0 °C. The reaction proceeded exclusively at the C(α)-position even in the presence of more acidic C–H bonds. A quaternary azaphosphonium cation, generated by the reaction between BINAP and DBAD followed by solvolytic *N*-chloromethylation, is proposed to be the active catalyst that reacts directly with the alkylpyridine substrate.

Introduction

Organophosphorus compounds have established their position as indispensable tools in synthetic organic chemistry, represented by their applications to Wittig, Horner-Wadsworth-Emmons, and Mitsunobu reactions.[1-5] Beyond their use as stoichiometric reagents, organophosphorus compounds have gained significant attention as metallomimetic catalysts,[6-8] offering the potential to replace or even surpass the reactivities of precious metal catalysts. In contrast to the conventional use of phosphines as Lewis base catalysts, cationic organophosphorus species, especially electrophilic phosphonium cations (EPCs), have exhibited potent activity as nonmetallic Lewis acid catalysts by leveraging their low-lying σ* orbital.[9-12] The versatility of EPCs as Lewis acids has been mainly demonstrated in a context of electrophile activation (Scheme 1a), promoting Diels-Alder reaction (dienophile activation),[13,14] Mukaiyama aldol reaction (C=O bond activation),[15-18] Mannich-type reaction (C=N bond activation),[14] and so on. One notable example is the EPC catalyst $[(C_6F_5)_3PF][B(C_6F_5)_4]$, developed by Stephan and co-workers, which enables functionalization of alkenes and alkynes (C=C and C≡C bond activation)[19,20] and even challenging defluorinative functionalization of alkylfluorides[21-23] through sp^3-C–F bond cleavage generating carbocation species under mild reaction conditions.[24,25] Despite these advances, the use of EPCs in direct C–H bond functionalization has been remarkably underexplored. While Greb and co-workers have demonstrated that highly Lewis acidic catecholato phosphonium ion can promote sp^2-C–H bond activation of thiophenes and pyrroles to form C–P bond, the transformations require stoichiometric amounts of phosphonium reagents (Scheme 1b).[26,27] Catalytic C–H bond transformations have been limited to substrates that have easily activatable sp^3-C–H protons of low pK_a values, such as nitromethane,[28] where the EPC catalyst facilitates deprotonation to generate nucleophilic species instead of activating electrophilic partners. The restricted application would be ascribed to the incompatibility of potent EPCs with general bases, whose combination greatly enhances the deprotonation of broad range of substrates. Thus, development of a potent and robust EPC catalysis capable of direct transformation of less activated sp^3-C–H bonds holds a promise for expanding their utility in synthetic organic chemistry, especially for late stage functionalization, but remains a significant challenge.[29-31]

Catalytic sp^3-C–H amination has been a subject of intense research in organic chemistry as a strategy for streamlining the synthesis of valuable nitrogen-containing molecules.[32-35] Among the various target substrates, 2-alkylpyridines are of great interest due to the prevalence of the pyridine motif in biologically relevant molecules, the most frequently used heterocyclic ring system in FDA-approved small-molecule drugs.[36,37] However, very few catalytic methods for C(α)–H amination of 2-alkylpyridines have been reported.[38,39] Moreover, the reported methods require high temperatures (>80 °C) and the use of transition metals (palladium or copper), hampering their application to multifunctional molecules such as pharmaceuticals. Herein, we report a phosphorus-catalyzed sp^3-C–H functionalization, enabling C(α)-selective amination of 2-alkylpyridines using di-*t*-butyl azodicarboxylate (DBAD) as an aminating reagent (Scheme 1c). The reaction proceeded under mild conditions at 0 °C, allowing site-selective sp^3-C–H amination of multi-substituted alkylpyridines including those found in pharmaceuticals. Furthermore, mechanistic investigations indicated that the actual active species is an

[a] *Department of Chemistry, Faculty of Science, Hokkaido University, Kita 10 Nishi 8, Kita-ku, Sapporo, Hokkaido 060-0810, Japan.*
[b] *Catalytic Chemistry Research Institute, National Institute of Advanced Industrial Science and Technology (AIST), Tsukuba, Ibaraki 305-8565, Japan.*
[c] *Institute for Catalysis, Hokkaido University, Kita 21, Nishi 10, Kita-ku, Sapporo 001-0021, Hokkaido, Japan.*
[d] *Institute for Chemical Reaction Design and Discovery (WPI-ICReDD), Hokkaido University, Kita 21 Nishi 10, Kita-ku, Sapporo, Hokkaido 001-0021, Japan.*
[e] *List Sustainable Digital Transformation Catalyst Collaboration Research Platform, Institute for Chemical Reaction Design and Discovery (ICReDD List-PF), Hokkaido University, Kita 21 Nishi 10, Kita-ku, Sapporo, Hokkaido 001-0021, Japan.*
†Supplementary Information available. See DOI: 10.1039/x0xx00000x

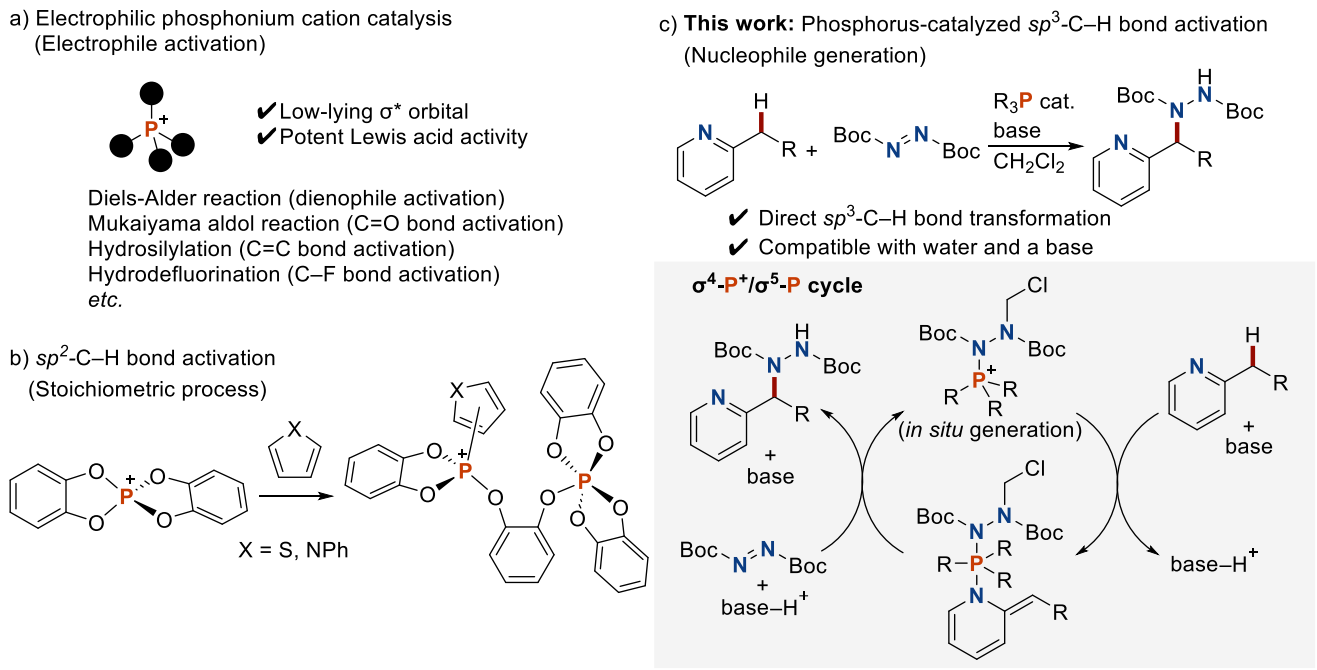

Scheme 1 Electrophilic Phosphonium Cations.

in situ generated electrophilic azaphosphonium cation that exhibits robustness toward water and base. Preliminary computational analyses suggest that a previously unrecognized intramolecular hydrogen bond contributes to the stability of the phosphonium cation.

Results and discussion

Discovery of phosphorus-catalyzed C(α)–H amination and effects of reaction parameters. In our exploration of transition metal-catalyzed *sp*^{3}-C–H transformations,[40] we found that *sp*^{3}-C–H amination of 2-methylpyridine (**1a**) with di-*t*-butyl azodicarboxylate (DBAD) was enabled by a catalytic amount of *rac*-BINAP (**P1**) in the presence of water and stoichiometric basic promoter Cs_2CO_3 in CH_2Cl_2 as a critical reaction solvent: no reaction occurred in other solvents such as THF, toluene, and acetonitrile (see Supporting Information for more details). Surprisingly, even 1,2-dichloroethane as a solvent caused no reaction. The reaction in CH_2Cl_2 proceeded cleanly and smoothly at room temperature in 3 h, affording **2a** in 99% yield (Table 1, entry 1). The temperature could be lowered to 0 °C without a significant drop in the yield by prolonging the time to 24 h (95% yield, entry 2). Characteristically, a catalyst aging period was indispensable for the reaction to occur efficiently. Thus, for the efficient production of **2a**, **P1** and DBAD were stirred in CH_2Cl_2 at 0 °C for 20 h prior to the addition of **1a**, Cs_2CO_3, and H_2O. Without this aging, the yield of **2a** dropped drastically to 10% (entry 3). The structure of the phosphine catalyst significantly affected the catalytic activity. Simpler bisphosphines, DPPE (**P2**) and DPPBz (**P3**), showed much lower catalytic activities, giving **2a** in only 10% and 22% yields, respectively (entries 4 and 5). XANTPHOS (**P4**), having a rigid tricyclic backbone, exhibited good activity but gave **2a** with a yield (70% yield) lower than **P1** (entry 6). The importance of the binaphthyl backbone of BINAP (**P1**) with extended aromatic systems was suggested by the low yield of 11% with biphenyl analogue **P5** (entry 7) and by the moderate yield of 64% with the partially saturated analogue **P6** (entry 8).

Simple monophosphines, Ph_3P (**P7**) and Cy_3P (**P8**), as well as a phosphite **P9** were poorly active, giving **2a** in less than 10% yields (Table 1, entries 9–11). As compared with these simple monophosphines, (1,1'-biphenyl-2-yl)diphenylphosphine **P10** showed a slightly better yield of 13% (entry 12). Introducing a 2',6'-dimethoxy substituent to the biphenyl moiety (**P11**) further increased the activity, affording **2a** in 31% yield (entry 13). Along this line, a notable increase in yield to 79% was observed with MOP (**P12**, entry 14), a monophosphine featuring a methoxy-substituted binaphthyl backbone. This observation clearly showed that having two phosphorus atoms is not essential for the activity of the phosphine catalyst precursor and that the MeO group may cause a favorable effect in the reaction with this functionalized monophosphine catalyst precursor.

It should be noted that H_2O and Cs_2CO_3 were both essential for achieving the high yield with the BINAP (**P1**) catalyst precursor; yields of **2a** were 6% without H_2O and 10% without Cs_2CO_3 (Table 1, entries 15 and 16). Even a catalytic amount of Cs_2CO_3 (20 mol%) exhibited significant impact on the yield, giving **2a** in 89% yield (entry 17).

Substrate scope. Having the optimized conditions in hand, the scope of 2-alkylpyridines was investigated at a 0.3 mmol-scale either at room temperature or at 0 °C, depending on the substrates (Scheme 2). The simplest product **2a** was isolated in excellent yield (96%) after purification by silica gel column chromatography. Moreover, the reaction was successfully conducted at a 2-mmol-scale, affording **2a** in 92% yield. Next, a series of lutidine-type substrates was examined to

Table 1 Effects of reaction parameters for sp^3-C–H amination of 2-methylpyridine[a]

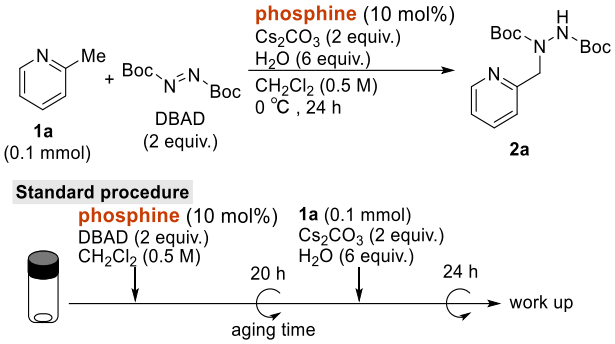

entry	phosphine	deviation from the original conditions	**2a** (%)
1	*rac*-BINAP (**P1**)	room temperature for 3 h	>99
2	**P1**	–	95
3	**P1**	without aging **P1** and DBAD in CH_2Cl_2	10
4	DPPE (**P2**)	–	10
5	DPPBz (**P3**)	–	22
6	XANTPHOS (**P4**)	–	70
7	**P5**	–	11
8	*rac*-H_8-BINAP (**P6**)	–	64
9	Ph_3P (**P7**)	–	3
10	Cy_3P (**P8**)	–	5
11	$(PhO)_3P$ (**P9**)	–	3
12	**P10**	–	13
13	**P11**	–	31
14	MOP (**P12**)	–	79
15	*rac*-BINAP (**P1**)	without H_2O	6
16	*rac*-BINAP (**P1**)	without Cs_2CO_3	10
17	*rac*-BINAP (**P1**)	20 mol% Cs_2CO_3	89

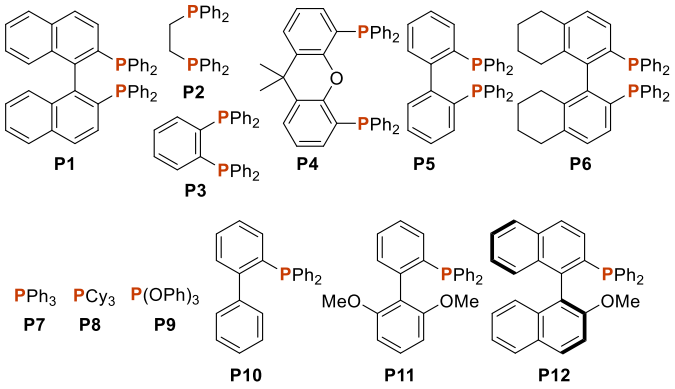

[a]Phosphine (0.01 mmol), DBAD (0.2 mmol), CH_2Cl_2 (200 µL, 0.5 M), 0 °C, 20 h; **1a** (0.1 mmol), Cs_2CO_3 (0.2 mmol), H_2O (0.6 mmol), 24 h. Yield was determined by ^1H NMR analysis using tetrachloroethane as the standard.

test the site selectivity of this reaction. The reaction of 2,3-lutidine (**1b**) occurred with exclusive selectivity at the 2-Me group, giving **2b** in quantitative yield. The reaction of 2,4-lutidine (**1c**) predominantly afforded **2c** in 78% yield along with a small amount of doubly aminated products: a diamine derivative resulting from amination at both the C2 and C4 methyl groups and an aminal formed by diamination at the C2-methyl group. 2,5-Lutidine (**1d**) showed good reactivity, producing **2d** as the sole product in 84% yield. In sharp contrast, 2,6-lutidine (**1e**) did not react at all, suggesting the sensitivity of the catalysis toward the steric hindrance around the nitrogen atom of the pyridine ring. 2,3,5-Collidine was also reactive, yielding **2f** in 97% yield.

Next, influences of various substituents on the pyridine ring were assessed. An electron-donating methoxy substituent at C4 position significantly increased the reactivity, affording doubly aminated aminal product **3g** in 86% yield (Scheme 2). The predominant formation of **3g** from **1g** indicates that increased Lewis basicity of the pyridine moiety by the 4-MeO group overrides the steric hindrance of the hydrazine group introduced by the first C–H amination, causing the second C–H amination. Halogen substituents at the C4 position were well-tolerated and the corresponding monoamination products were obtained in good yields (**2h**, 84%; **2i**, 74%). Regarding substitution at the C5 position, an ethyl group (**1j**) slightly decreased the yield compared to 2,5-lutidine (**2j**, 56% vs. **2d**, 84%), indicating significant sensitivity of this reaction to steric demand around this position. A substrate (**1k**) bearing a methoxycarbonyl group was compatible (**2k**, 72%), while the highly electron-withdrawing nitro group of **1l** inhibited the reaction significantly (**2l**, 12%).

The catalysis was also applicable to the amination of secondary C–H bonds (Scheme 2). The reaction of 2-ethylpyridine **1m** gave branched alkylamine derivative **2m** in moderate yield (45%). Longer alkyl chains such as propyl (**1n**) and pentyl (**1o**) groups were tolerated at the pyridine C2 position, providing C(α)-amination products selectively (**2n**, 63%; **2o**, 20%). The exclusive regioselectivity was retained even when another benzylic position was present in the substrate (**2p**, 28%). In addition to simple alkyl chains, phenyl (**1q**) and methoxycarbonyl (**1r**) groups were also acceptable at the C(α)-

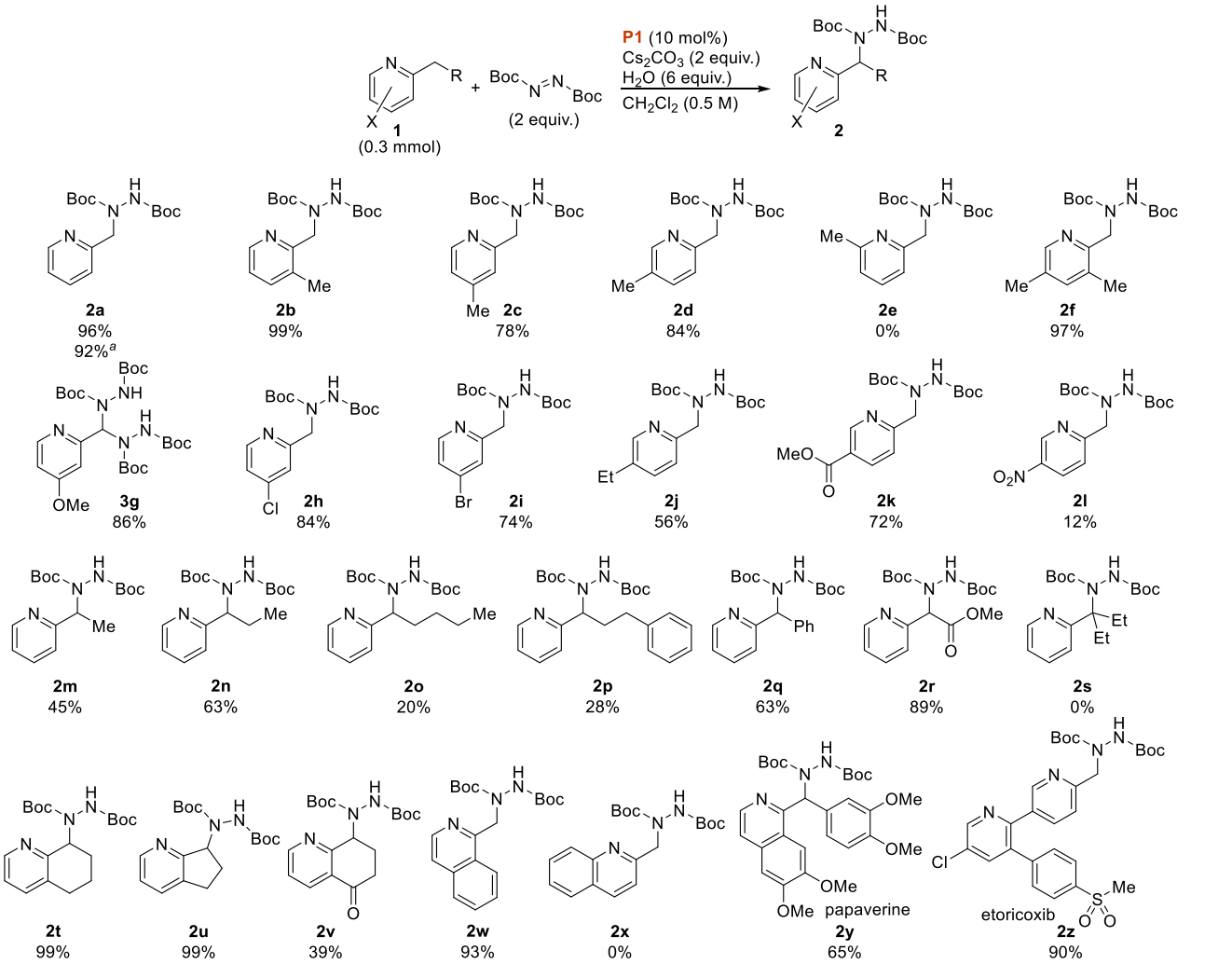

Scheme 2 Phosphine-catalyzed C(α)-amination of 2-alkylpyridines. **1** (0.3 mmol), DBAD (0.6 mmol), **P1** (0.03 mmol) CH_2Cl_2 (600 μL, 0.5 M), Cs_2CO_3 (0.6 mmol), H_2O (1.8 mmol). Stirring at 0 °C for 24 h or at room temperature for 3 h. Yields of the isolated products are reported. [a]2 mmol-scale reaction.

position (**2q**, 63%; **2r**, 89%). However, **1s** with a sterically demanding tertiary C(α)–H was intact under the conditions. Bicyclic alkyl pyridines, fused with a six- or a five-membered ring, exhibited high reactivity, giving **2t** and **2u**, respectively, in quantitative yield. Notably, for substrate **1v** with a keto group, the amination occurred at the position α to the pyridine ring, even in the presence of inherently more acidic sp^3-C–H bonds adjacent to the ketonic carbonyl group (**2v**, 39% yield). In addition to the 2-alkylpyridines, 1-methylisoquinoline (**1w**) reacted to give **2w** in 93% yield, but 2-methylquinoline (**1x**) was unreactive, likely due to the steric hindrance around the nitrogen atom. Although extension of the catalysis to an enantioselective variant is conceivable, use of chiral (*R*)-BINAP did not work for this purpose, giving racemic product **2t** from **1t**.

Since the pyridine ring is prevalent in biologically relevant molecules, the applicability of the catalytic system toward direct transformation of pharmaceuticals is of great interest. To our delight, both papaverine (**1y**), an antispasmodic agent, and etoricoxib (**1z**), a COX-2 inhibitor, successfully participated in this C–H amination to give the corresponding aminated products in good to high yields (Scheme 2, **2y**, 65%; **2z**, 90%). Notably, the methanesulfonyl group in etoricoxib remained intact, despite the marked acidity of the α-C–H bond of the sulfonyl group.

Transformations of the products. The utility of the C–H amination products was demonstrated by the following transformations (Scheme 3). First, the N–N bond in the product **2a** was cleaved through a two-step protocol, *N*-alkylation using α-bromo acetate followed by E1cB eliminative N–N bond cleavage, affording Boc-protected amine **5a** in 63% yield.[41] The same protocol was applicable to **2t**, affording α-branched amine **5t** in 75% yield. The hydrazine moiety of **2a** could be used for the synthesis of an azaheterocyclic compound. Thus, after Boc-deprotection for **2a** with TFA, the resulting hydrazine **6** underwent a double condensation reaction with 2-chloro-3-ethoxycarbonylpyridine in the presence of triethylamine to produce **7** in 37% yield.

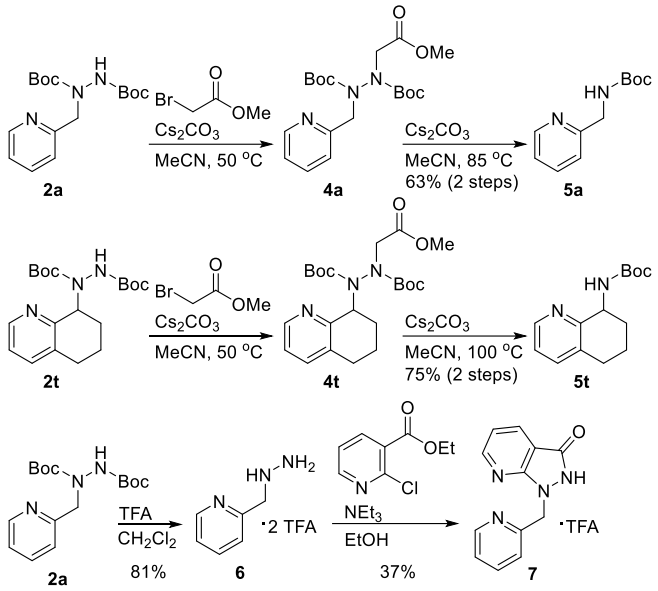

Scheme 3 Transformation of the products.

Kinetic experiments. To gain mechanistic insights into the C–H activation step, experiments using deuterated substrate **1a-D** were carried out (Scheme 4). When **1a-D** was subjected to the standard conditions, the yield of the aminated product dropped to 36% with full retention of deuterium atoms at the C(α)-position. The kinetic isotope effect (KIE) was evaluated by an intermolecular competition method using a 1:1 mixture of **1a** and **1a-D**. The observed KIE value was 6.2, indicating that the C–H activation step critically influenced the overall reaction rate.[42] In addition, the reaction kinetics were first order in **P1** and **1a**, while the concentration of DBAD did not affect the rate. These results suggest that the C–N bond formation with DBAD occurs after the rate-determining step. This is consistent with the observation of the large KIE value indicating that the C–H activation step is rate-determining.

Identification of catalytically active species. To obtain insights into the catalytically active organophosphorus species, the structural changes of the catalyst precursor *rac*-BINAP (**P1**) upon addition of the reagents (DBAD, Cs_2CO_3, H_2O) and substrate **1a** were monitored by ^{31}P NMR spectroscopy (Fig 1). Upon adding DBAD to a solution of **P1** in CH_2Cl_2 at 0 °C, several new representative signals appeared, including a broad signal at δ 42.5 ppm and a signal at δ –17.9 ppm attributable to Mitsunobu-type betaine **P1**$^+$**NN**$^-$ (indicated by pink-filled boxes in Fig. 1a); the former is assigned to the quaternalized positively charged P atom and the latter to the tertiary neutral P atom.[43] The signals for **P1**$^+$**NN**$^-$ (δ 42.5 and –17.9 ppm) gradually decreased (see the spectrum at 6 h) and disappeared at 20 h, which corresponds to the catalyst aging period for the optimal C–H amination protocol. Simultaneously, the signals at δ 53.5, 50.9, and –17.4 ppm, which appeared initially as minor signals (indicated by red-filled circles and green-filled triangles), increased in intensity during the aging period. While the

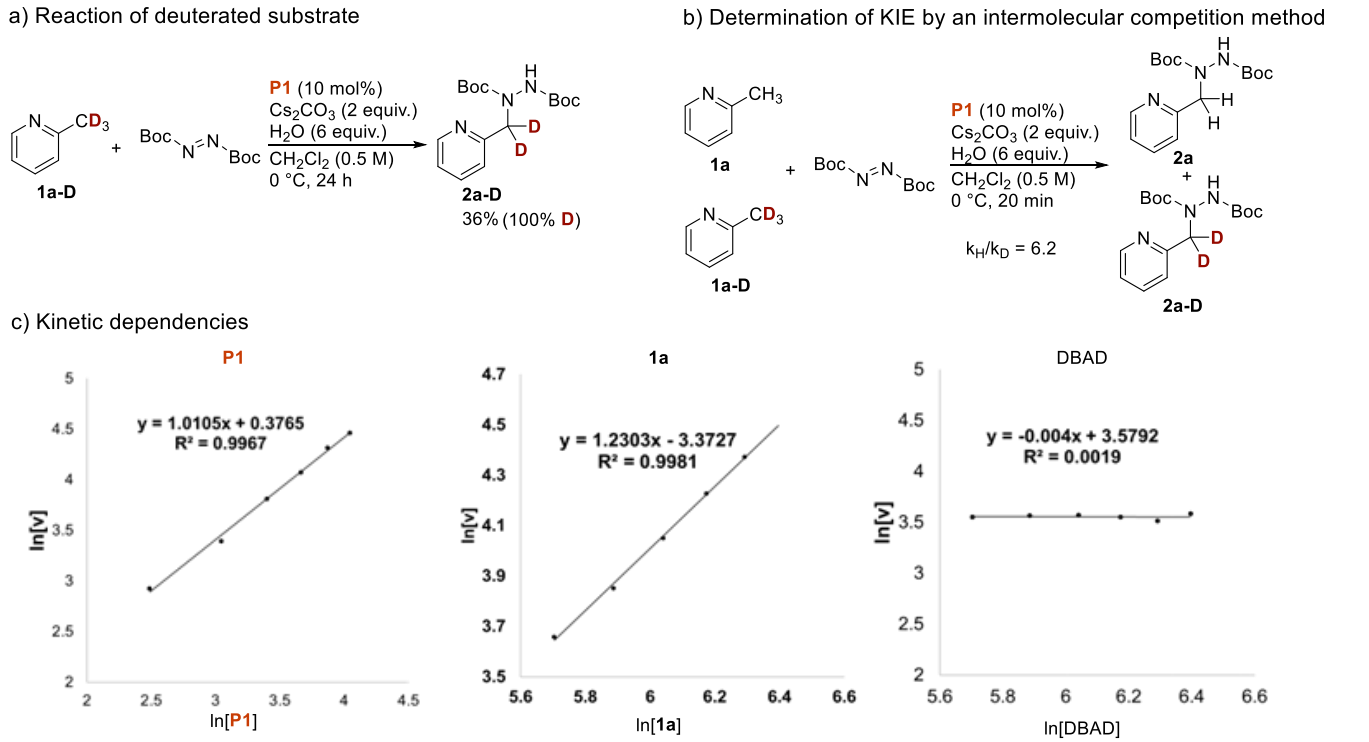

Scheme 4 Deuterium-labeling and kinetic experiments. a) **P1** (0.01 mmol), DBAD (0.2 mmol), CH_2Cl_2 (200 µL, 0.5 M), 0 °C, 20 h; **1a-D** (0.1 mmol), Cs_2CO_3 (0.2 mmol), H_2O (0.6 mmol), 24 h. b) **P1** (0.01 mmol), DBAD (0.2 mmol), CH_2Cl_2 (200 µL, 0.5 M), 0 °C, 20 h; **1a** (0.05 mmol), **1a-D** (0.05 mmol), Cs_2CO_3 (0.2 mmol), H_2O (0.6 mmol), 24 h. c) The reactions were conducted with **P1** (0.03 mmol), **1a** (0.3 mmol), and DBAD (0.6 mmol) as the standard reaction scale, and the amount of each reagent was varied to determine the kinetic dependencies.

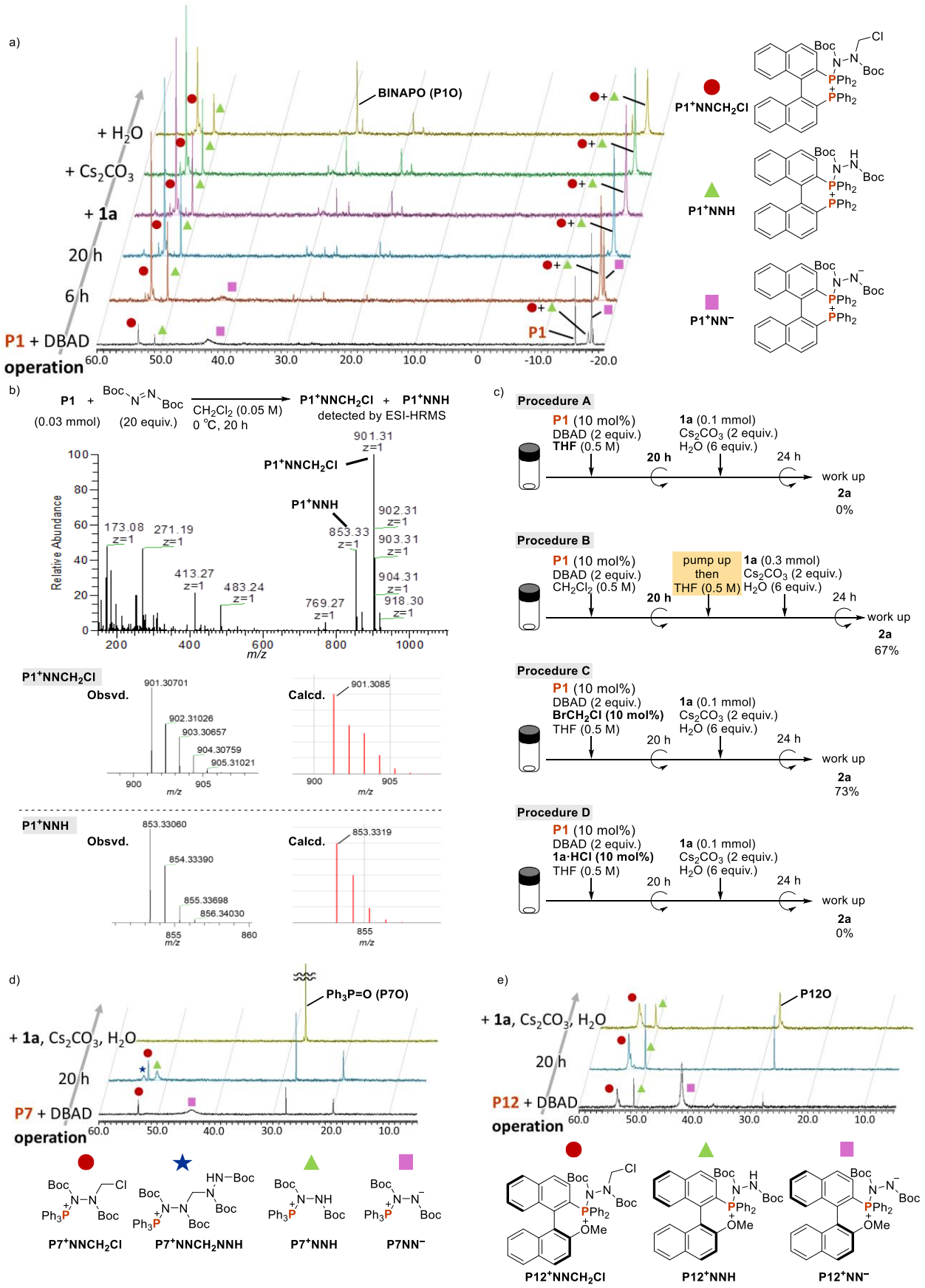

Fig. 1. a) ^{31}P NMR spectra using *rac*-BINAP (**P1**). b) ESI-HRMS analysis using *rac*-BINAP (**P1**). c) Experiments to identify catalytically active species. d) ^{31}P NMR spectra using PPh_3 (**P7**). e) ^{31}P NMR spectra using MOP (**P12**).

successive additions of **1a**, Cs_2CO_3, and H_2O caused a gradual increase of the signal at δ 28.2, which is assigned to the catalytically inactive bisphosphine dioxide of **P1** (BINAPO, **P1O**), the three major signals (δ 53.5, 50.9, and –17.4 ppm) remained unchanged. Finally, the C–H amination product **2a** was produced in the NMR sample in 74% yield after 24 h. These results suggested that the Mitsunobu-type betaine **P1$^+$NN$^-$** was converted into two different monoquaternalized bisphosphine species; one corresponds to the signals indicated by the green-filled triangles and the other by the red-filled circles. To identify the chemical structures of the assumed monoquaternalized bisphosphine species, ESI-HRMS analysis was performed on a sample prepared by stirring a solution of **P1** and DBAD (1:20) in CH_2Cl_2 (0.05 M) at 0 °C for 20 h before diluting with MeOH (Fig. 1b). The mass spectrum showed two strong signals at *m/z* 901.3070 corresponding to **P1$^+$NNCH$_2$Cl** (calcd. *m/z* 901.3085) and *m/z* 853.3306 corresponding to **P1$^+$NNH** (calcd. *m/z* 853.3319). Formation of these **P1$^+$NNCH$_2$Cl** and **P1$^+$NNH** species can be explained by the reactions of Mitsunobu-type betaine **P1$^+$NN$^-$** with the solvent CH_2Cl_2 and residual water, respectively. In both cases, only one of the two P atoms of the bisphosphine (**P1**) reacted to form a phosphonium cation, while the other remained intact. Based on these ESI-HRMS observations, the major ^{31}P NMR signals at δ 53.5 (red-filled circles) and 50.9 ppm (green-filled triangles) can be assigned to phosphonium P$^+$ of **P1$^+$NNCH$_2$Cl** and **P1$^+$NNH**, respectively.[44] The signals for neutral P of these species overlap at δ –17.4 ppm.

To identify which is the catalytically active species, **P1$^+$NNCH$_2$Cl** or **P1$^+$NNH**, and to determine how the chloromethylated species is produced, the *sp*^{3}-C–H amination reactions were conducted with modified procedures using **1a** as the substrate (Fig. 1c). When the solvent was changed from CH_2Cl_2 to THF for the standard procedure (Procedure A), no reaction occurred. In sharp contrast, when the solvent was replaced by THF after the aging time, during which **P1** (10 mol%) and DBAD (2 equiv.) were stirred for 20 h in CH_2Cl_2 (Procedure B), **2a** was obtained in 67% yield. These results indicate that CH_2Cl_2 plays a critical role not only as a solvent but also as an *N*-alkylating agent for the Mitsunobu-type betaine **P1$^+$NN$^-$** to generate **P1$^+$NNCH$_2$Cl** as the catalytically active species. In addition, when 10 mol% of $BrCH_2Cl$ (1 equiv to **P1**) was used as an additive in THF, expecting the formation of **P1$^+$NNCH$_2$Cl** (Procedure C), **2a** was obtained in a yield (73%) comparable to that with Procedure B. On the other hand, the addition of a catalytic amount of **1a**·HCl salt to facilitate the formation of protonated **P1$^+$NNH** resulted in no product formation (Procedure D). Based on these results on the effects of the *N*-alkylating agents, we conclude that the *N*-chloromethylated **P1**-DBAD adduct **P1$^+$NNCH$_2$Cl** is the catalytically active species for the *sp*^{3}-C–H amination with **P1** as a catalyst precursor.[45]

For comparison, the ^{31}P NMR experiment using the inefficient catalyst precursor PPh_3 (**P7**) was investigated (Fig. 1d, see Supporting Information for details). In this case, triphenylphosphine oxide **P7O** (28 ppm), betaine **P7$^+$NN$^-$** (44 ppm, pink-filled boxes), one phosphonium species (53 ppm, red-filled circles), and an unassignable signal at 19 ppm were observed at the initial stage. After 20 h, the peak for **P7$^+$NN$^-$** disappeared, and two new signals (blue-filled stars and green-filled triangles) attributable to phosphonium cations appeared at a lower magnetic field (δ 50–55 ppm). In contrast to the case with *rac*-BINAP (**P1**), these three phosphonium cation species completely disappeared upon addition of **1a**/Cs_2CO_3/H_2O, leaving only **P7O**. The disappearance of the phosphonium-derived signals indicates their instability. This is in accord with the poor performance of **P7** for the C–H amination. In addition, ESI-HRMS analysis of a sample prepared following the same protocol as for the corresponding **P1** sample exhibited only a very weak signal attributable to **P7$^+$NNCH$_2$Cl**. Instead, a strong signal corresponding to a species with a 1,1-di(hydrazyl)methane moiety (**P7$^+$NNCH$_2$NNH**, calcd. *m/z* 737.3674, obsvd. *m/z* 737.3652) was observed after 20 h of aging along with **P7$^+$NNH** as one of the prominent species (see Supporting Information). The formation of **P7$^+$NNCH$_2$NNH** is likely due to the reaction of **P7$^+$NNCH$_2$Cl** with **P7$^+$NN$^-$**, followed by hydrolysis by the residual water, resulting in concomitant formation of **P7O**. This degradation of **P7$^+$NNCH$_2$Cl**, which may potentially be a catalytically active species, leading to **P7O** is likely a major reason for the inefficiency of the simple monophosphine Ph_3P (**P7**) as a catalyst precursor.

Interestingly, the ^{31}P NMR experiment and ESI-HRMS analysis using the competent monophosphine catalyst precursor MOP (**P12**) exhibited a trend similar to that observed with *rac*-BINAP (**P1**) (Fig. 1e and Supporting Information). This suggests good stability of the catalytically active *N*-alkylated species **P12$^+$NNCH$_2$Cl** (calcd. *m/z* 747.2749, obsvd. *m/z* 747.2739), while unassignable ^{31}P NMR signals in the region corresponding to phosphonium cation species (δ 50–55 ppm) were observed. The sharp contrast between the two monophosphines, Ph_3P (**P7**) and MOP (**P12**), suggests the contributions of the binaphthyl scaffold and the pendant methoxy group in MOP (**P12**) in enhancing the stability of the catalytically active species.

Proposed catalytic cycle. Based on the experimental results, the following catalytic mechanism is proposed for the phosphorus-catalyzed C(α)-selective *sp*^{3}-C–H amination of 2-alkylpyridines (Scheme 5). Initially generated Mitsunobu-type betaine intermediate **P$^+$NN$^-$** is alkylated by dichloromethane *in situ* during the aging period, providing azaphosphonium salt **P$^+$NNCH$_2$Cl**·Y$^-$ (σ^4-P$^+$) as the active species. This azaphosphonium salt forms an association complex **A** with 2-alkylpyridine substrate **1** as suggested by DFT calculations discussed later. The formation of a stable P–N coordination intermediate is unlikely based on the ^{31}P NMR observation that the addition of the 2-alkylpyridine caused virtually no influence on the chemical shift of the phosphonium species (Fig. 1a). Next, deprotonation of a C(α)-proton of **A** by the counteranion (Y$^-$) of the azaphosphonium cation is associated with concomitant interaction of the developing aza anion with the cationic phosphorus center of the azaphosphonium species (**TS$_{A\text{-}B}$**), resulting in the formation of a pentavalent diazatriorganophospholane (**B**, σ^5-P) with an enamide substituent.[40] Based on the results of the kinetic studies (Scheme 4), this concerted deprotonation step is most likely the

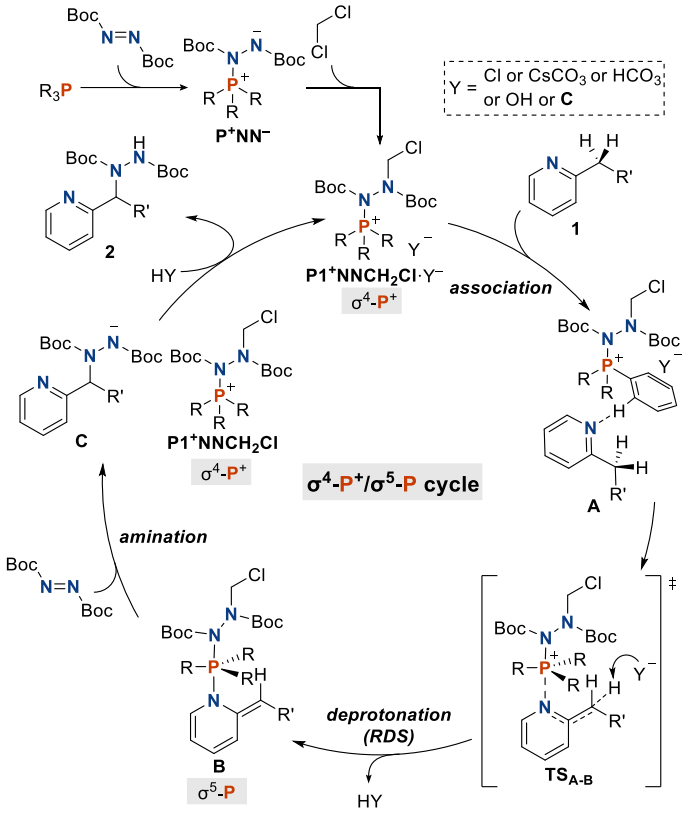

Scheme 5 Proposed catalytic cycle.

rate determining step of the catalytic reaction. Subsequently, the enamide **B** undergoes nucleophilic addition to the N–N double bond of DBAD to form the C(α)–N bond, generating an ion pair between the anionic addition product **C** and azaphosphonium ion **P⁺NNCH₂Cl**. Finally, protonation of **C** with the HY species affords the C(α)–H amination product **2** with regeneration of azaphosphonium salt **P⁺NNCH₂Cl**·Y⁻ (σ^4-P⁺) to close the catalytic cycle. Based on this catalytic cycle, water and Cs_2CO_3 may play roles in facilitating the protonation (**C** to **2**) and deprotonation (**A** to **B**), respectively.

Computational studies. To gain three-dimensional molecular insight into the proposed mechanism, density functional theory (DFT) calculations were performed for exploring the natures of the three catalytic intermediates, azaphosphonium cation **P1⁺NNCH₂Cl**, association complex **A**, and enamide **B**, for the sp^3-C–H amination of 2-methylpyridine (**1a**) with di-*t*-butyl azodicarboxylate (DBAD) promoted by the most efficient catalyst precursor *rac*-BINAP (**P1**) at the ωb97X-D/6-31G+(d,p) level of theory (Fig. 2).

The optimized **P1⁺NNCH₂Cl** adopts a pseudo trigonal pyramidal geometry around the P⁺ center, providing substantial room-for the pyridine substrate to approach the P⁺ center from the side opposite to the apical N atom (Fig. 2a). Noncovalent interaction (NCI) analysis by the independent gradient model based on the Hirshfeld partition (IGMH) method[46] using the Multiwfn program[47] indicates the existence of an sp^3-C–H···P nonclassical hydrogen bond between the P atom of the appended phosphine moiety and the methylene C–H bond of the *N*-chloromethyl group, suggesting that this interaction may contribute to the enhanced stability of this species relative to the corresponding species produced from more simple phosphine PPh_3 (**P7**), which was shown in the ^{31}P NMR experiments [Fig. 1 a) vs. d)]. As is common with BINAP derivatives, a π/π-stacking interaction between the appended naphthalene ring and one of the P-phenyl groups of **P1** is observed.

All the attempts to locate a complex resulting from the coordination of the pyridine N atom of **1a** to the P⁺ center of **P1⁺NNCH₂Cl** failed but instead led to identification of an association complex (**A-P1-1a**) between **P1⁺NNCH₂Cl** and **1a** as a precursor for deprotonation of the C(α)–H bond (Fig. 2b). According to NCI analysis, a sp^2-C–H···N nonclassical hydrogen bond between one of the *P*-Ph *ortho*-C–H bonds and the pyridine N atom seems to be the primary attractive interaction of the association complex, while mutual multiple C–H/π interactions between the pyridine ring of **1a** and the naphthalene rings of **P1** may also contribute to stabilization of the complex.

The exploration of a transition state for the subsequent deprotonation to form an enamide intermediate was challenging primarily due to uncertainty of the counteranion (Y^-: Cl^-, $CsCO_3^-$, HCO_3^-, HO^-, or **C**), which serves as a Brønsted base. Instead, an N-to-P-coordinated enamide intermediate (**B-P1-1a**) with a trigonal bipyramidal phosphorus geometry (σ^5-**P**) was identified as a reasonable deprotonation product in accord

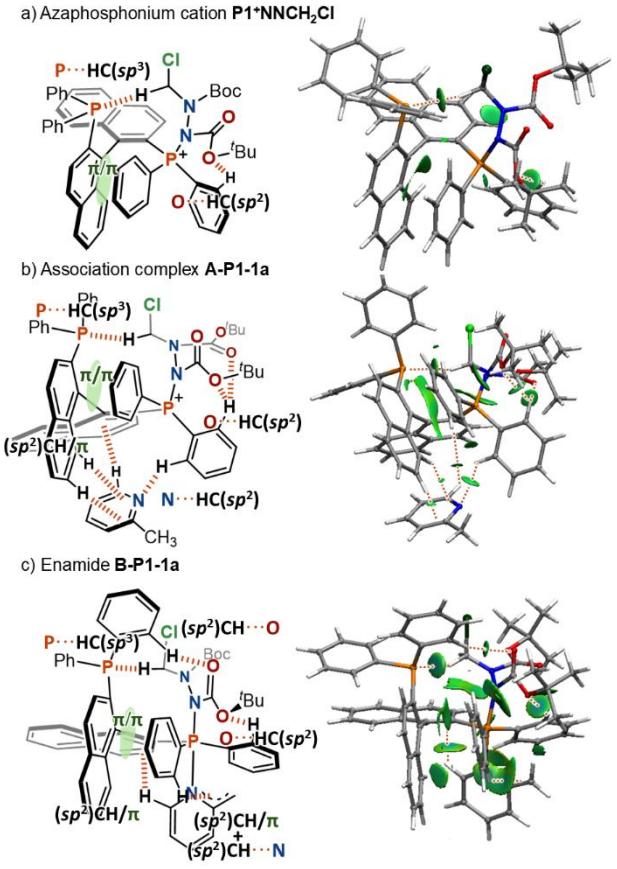

Fig. 2 Calculated structures of key intermediates.

with the assumed association of the N···P^+ interaction in the deprotonative transition state ($TS_{A\text{-}B}$ in Scheme 5) (Fig. 2c). The sp^3-C–H···P hydrogen bond donated by the *N*-chloromethyl group is retained in this species. Additionally, a sp^2-C–H···O hydrogen bond is formed between one of the *P*-phenyl *ortho*-C–H bonds of the appended diphenylphosphino group and one of the Boc carbonyl oxygen atoms. This attractive interaction caused by the appended phosphine moiety may also contribute to the better performance of the bisphosphine-type catalyst precursors such as **P1** as compared to the monophosphine-types.

Although the reason for the superior performances of the functionalized phosphines as compared to those of more simple phosphines as catalyst precursors is not clear, it may be related to the noncovalent interactions caused by the appended functional groups including the sp^3-C–H···P hydrogen bond retained throughout the catalytic cycle and the sp^2-C–H···O hydrogen bond observed in the enamide intermediate–σ^5-P intermediate (**B-P1-1a**) as well as the π/π and C–H/π interactions. Concerning the stereoselectivity of this C–H amination, the C(α) reacting site of the enamide–σ^5-P intermediate (**B-P1-1a**) is located far beyond the area where the steric effects of the intermediate can be influential, explaining the lack of enantioselectivity when these particular catalyst precursors were employed. Thus, more sophisticated phosphorus molecules must be designed for applying this reaction to enantioselective transformations.

Conclusions

We have developed a phosphorus-catalyzed C(α)-selective sp^3-C–H amination of 2-alkylpyridines as an unprecedented example of a sp^3-C–H functionalization catalyzed by an organophosphorus compound. The reaction proceeded under exceptionally mild conditions at 0 °C with H_2O and Cs_2CO_3 as promoters. Mechanistic investigations suggested that the catalytically active species is an azaphosphonium cation generated by the reaction of a phosphine and DBAD and subsequent solvolytic *N*-chloromethylation in CH_2Cl_2. It is proposed that the rate-determining sp^3-C–H activation step is facilitated by the coordination of the pyridine to the cationic phosphorus center. The versatility of the method was demonstrated by applying it to the direct and site-selective amination of pharmaceuticals, retaining inherently more acidic sp^3-C–H bonds. Efforts to realize enantioselective phosphorus catalysis based on the knowledge obtained in this work are underway in our laboratory.

Author contributions

M. S. and Y. S. conceived the project. A. Y., M. S. and Y. S. directed the project. Y. H. performed all the experiments and A. T. and K. N.-K. contributed to determine the optimal reaction conditions. Y. H. and Y. S. analysed and characterised all compounds. Y. H. performed theoretical calculations. All authors were involved in reviewing and editing the manuscript.

Conflicts of interest

There are no conflicts to declare.

Data availability

The data supporting this article have been included as part of the Supplementary Information.

Acknowledgements

This work was supported by the Institute for Chemical Reaction Design and Discovery (WPI-ICReDD) and Hokkaido University as well as JSPS KAKENHI No. JP22K19016, No. JP22H05329 (Digi-TOS), No. JP24H01828 (Green Catalysis Science) to YS, No. JP21H04680 to MS, No. JP21H05224 (Digi-TOS) to AY and No. JP23KJ0022 to YH. YS also acknowledges JST PRESTO (JPMJPR24M4), THE AKIYAMA LIFE SCIENCE FOUNDATION and financial support from ICReDD List-PF.

Notes and references

1 M. M. Heravi, V. Zadsirjan, M. Daraie and M. Ghanbarian, Applications of Wittig Reaction in the Total Synthesis of Natural Macrolides, *ChemistrySelect*, **2020**, *5*, 9654–9590.
2 D. Roman, M. Sauer and C. Beemelmanns, Applications of the Horner–Wadsworth–Emmons Olefination in Modern Natural Product Synthesis, *Synthesis*, **2021**, *53*, 2713–2739.
3 K. Kobayashi, K. Tanaka and H. Kogen, Recent Topics of the Natural Product Synthesis by Horner–Wadsworth–Emmons Reaction, *Tetrahedron Lett.*, **2018**, *59*, 568–582.
4 S. Munawar, A. F. Zahoor, S. Ali, S. Javed, M. Irfan, A. Irfan, K. Kotwica-Mojzych and M. Mojzych, Mitsunobu Reaction: A Powerful Tool for the Synthesis of Natural Products: A Review, *Molecules*, **2022**, *27*, 6953.
5 K. C. K. Swamy, N. N. B. Kumar, E. Balaraman and K. V. P. P. Kumar, Mitsunobu and Related Reactions: Advances and Applications, *Chem. Rev.*, **2009**, *109*, 2551–2651.
6 J. M. Lipshultz, G. Li and A. T. Radosevich, Main Group Redox Catalysis: Reversible PIII/PV Redox Cycling at a Single Phosphorus Center, *J. Am. Chem. Soc.*, **2021**, *143*, 1699–1721.
7 L. Longwitz and T. Werner, Recent Advances in Phosphonium Salt Organocatalysis, *Pure Appl. Chem.*, **2019**, *91*, 95–102.
8 C. Xie, G. Chen, C.-G. Feng, G.-Q. Lin and R. Hong, Recent Advances in Asymmetric P(III)/P(V)=O Redox Catalysis, *Tetrahedron Lett.*, **2024**, *152*, 155337.
9 J. M. Bayne and D. W. Stephan, Phosphorus Lewis Acids: Emerging Reactivity and Applications in Catalysis, *Chem. Soc. Rev.*, **2016**, *45*, 765–774.
10 T. Werner, Phosphonium Salt Organocatalysis, *Adv. Synth. Catal.*, **2009**, *351*, 1469–1481.
11 D. W. Stephan, A Tale of Two Elements: The Lewis Acidity/Basicity Umpolung of Boron and Phosphorus, *Angew. Chem., Int. Ed.*, **2017**, *56*, 5984–5992.
12 O. Sereda, S. Tabassum and R. Wilheim, Lewis Acid Organocatalysts, *Top. Curr. Chem.*, **2009**, *291*, 349–393.
13 M. Terada and M. Kouchi, Novel Metal-free Lewis Acid Catalysis by Phosphonium Salts through Hypervalent Interaction, *Tetrahedron*, **2006**, *62*, 401–409.
14 M. Vogler, L. Süsse, J. H. W. LaFortune, D. W. Stephan and M. Oestreich, Electrophilic Phosphonium Cations as Lewis Acid Catalysts in Diels–Alder Reactions and Nazarov Cyclizations, *Organometallics*, **2018**, *37*, 3303–3313.

15 T. Mukaiyama, K. Kashiwagi and S. Matsui, A Convenient Synthesis of β-Aminoesters. The Reaction of Imines with Ketene Silyl Acetals Catalyzed by Phosphonium Salts, *Chem. Lett.*, **1989**, *18*, 1397–1400.

16 T. Mukaiyama, S. Matsui and K. Kashiwagi, Effective Activation of Carbonyl and Related Compounds with Phosphonium Salts. The Aldol and Michael Reactions of Carbonyl Compounds with Silyl Nucleophiles and Alkyl Enol Ethers, *Chem. Lett.*, **1989**, *18*, 993–996.

17 A. Bohsako, C. Asakura and T. Shioiri, Tetraphenylphosphonium Hydrogendifluoride: A New Catalyst for Silyl-mediated Aldol Reaction and the Addition of Silylacetylenes to Carbonyl Compounds, *Synlett*, **1995**, *1995*, 1033–1034.

18 A. G. Barrado, J. M. Bayne, T. C. Johnstone, C. W. Lehmann, D. W. Stephan and M. Alcarazo, Dicationic Phosphonium Salts: Lewis Acid Initiators for the Mukaiyama–Aldol Reaction, *Dalton Trans.*, **2017**, *46*, 16216–16227.

19 M. Pérez, L. J. Hounjet, R. Dobrovetsky and D. W. Stephan, Olefin Isomerization and Hydrosilylation Catalysis by Lewis Acidic Organofluorophosphonium Salts, *J. Am. Chem. Soc.*, **2013**, *135*, 18308–18310.

20 M. Pérez, T. Mahdu, L. J. Hounjet and D. W. Stephan, Electrophilic Phosphonium Cations Catalyze Hydroarylation and Hydrothiolation of Olefins, *Chem. Commun.*, **2015**, *51*, 11301–11304.

21 C. B. Caputo, L. J. Hounjet, R. Dobrovetsky and D. W. Stephan, Lewis Acidity of Organofluorophosphonium Salts: Hydrodefluorination by a Saturated Acceptor, *Science*, **2013**, *341*, 1374–1377.

22 J. Zhu, M. Pérez, C. B. Caputo and D. W. Stephan, Use of Trifluoromethyl Groups for Catalytic Benzylation and Alkylation with Subsequent Hydrodefluorination, *Angew. Chem., Int. Ed.*, **2016**, *55*, 1417–1421.

23 J. Zhu, M. Pérez and D. W. Stephan, C–C Coupling of Benzyl Fluorides Catalyzed by an Electrophilic Phosphonium Cation, *Angew. Chem., Int. Ed.*, **2016**, *55*, 8448–8451.

24 M. Pérez, Z. W. Qu, C. B. Caputo, V. Podgorny, L. J. Hounjet, A. Hansen, R. Dobrovetsky, S. Grimme and D. W. Stephan, Hydrosilylation of Ketones, Imines and Nitriles Catalysed by Electrophilic Phosphonium Cations: Functional Group Selectivity and Mechanistic Considerations, *Chem. Eur. J.*, **2015**, *21*, 6491–6500.

25 M. Pérez, C. B. Caputo, R. Dobrovetsky and D. W. Stephan, Metal-free Transfer Hydrogenation of Olefins via Dehydrocoupling Catalysis, *Proc. Natl. Acad. Sci. U. S. A.*, **2014**, *111*, 10917–10921.

26 D. Roth, J. Stirn, D. W. Stephan and L. Greb, Lewis Superacidic Catecholato Phosphonium Ions: Phosphorus–Ligand Cooperative C–H Bond Activation, *J. Am. Chem. Soc.*, **2021**, *143*, 15845–15851.

27 D. Roth, A. T. Radosevich and L. Greb, Reversible Oxidative Addition of Nonactivated C–H Bonds to Structurally Constrained Phosphenium Ions, *J. Am. Chem. Soc.*, **2023**, *145*, 24184–24190.

28 J. McNulty, J. Dyck, V. Larichev, A. Capretta and A. J. Robertson, Phosphonium Salt Catalyzed Henry Nitroaldol Reactions, *Lett. Org. Chem.*, **2004**, *1*, 137–139.

29 V. Fasano, J. H. W. LaFortune, J. M. Bayne, M. J. Ingleson and D. W. Stephan, Air- and Water-Stable Lewis Acids: Synthesis and Reactivity of P-Trifluoromethyl Electrophilic Phosphonium Cations, *Chem. Commun.*, **2018**, *54*, 662–665.

30 J. M. Bayne, V. Fasano, K. M. Szkop, M. J. Ingleson and D. W. Stephan, Phosphorous(V) Lewis Acids: Water/Base Tolerant P_3-Trimethylated Trications, *Chem. Commun.*, **2018**, *54*, 12467–12470.

31 J. C. Glihula and A. T. Radosevich, Tetragonal Phosphorus(V) Cations as Tunable and Robust Catalytic Lewis Acids, *Chem. Sci.*, **2019**, *10*, 7177–7182.

32 D. Hazelard, P.-A. Nocquet and P. Compain, Catalytic C–H Amination at Its Limits: Challenges and Solutions, *Org. Chem. Front.*, **2017**, *4*, 2500–2521.

33 Y. Park, Y. Kim and S. Chang, Transition Metal-Catalyzed C–H Amination: Scope, Mechanism, and Applications, *Chem. Rev.*, **2017**, *117*, 9247–9301.

34 H. Hayashi and T. Uchida, Nitrene Transfer Reactions for Asymmetric C–H Amination: Recent Development, *Eur. J. Org. Chem.*, **2020**, 909–916.

35 H. Noda, X. Tang and M. Shibasaki, Catalyst-Controlled Chemoselective Nitrene Transfers, *Helv. Chim. Acta*, **2021**, *104*, e2100140.

36 J. Shearer, J. L. Castro, A. D. G. Lawson, M. MacCoss and R. D. Taylor, Rings in Clinical Trials and Drugs: Present and Future, *J. Med. Chem.*, **2022**, *65*, 8699–8712.

37 P. Bhutani, G. Joshi, N. Raja, N. Bachhav, P. K. Rajanna, H. Bhutani, A. T. Paul and R. Kumar, U.S. FDA Approved Drugs from 2015–June 2020: A Perspective, *J. Med. Chem.*, **2021**, *64*, 2339–2381.

38 J.-Y. Liu, H.-Y. Niu, S. Wu, G.-R. Qu and H.-M. Guo, Metal-Catalyzed C(sp^3)–H Bond Amination of 2-Alkyl Azaarenes with Diethyl Azodicarboxylate, *Chem. Commun.*, **2012**, *48*, 9723–9725.

39 B. Qian, L. Yang and H. Huang, Cu-Catalyzed Direct C–H Amination of 2-Alkylazaarenes with Azodicarboxylates via Nucleophilic Addition, *Tetrahedron Lett.*, **2013**, *54*, 711–714.

40 R. Murakami, K. Sano, T. Iwai, T. Taniguchi, K. Monde and M. Sawamura, Palladium-Catalyzed Asymmetric C(sp^3)–H Allylation of 2-Alkylpyridines, *Angew. Chem., Int. Ed.*, **2018**, *57*, 9465–9469.

41 P. Magnus, N. Negar Garizi, K. A. Seibert and A. Ornholt, Synthesis of Carbamates from Diethoxycarbonyl Hydrazine Derivatives by E1cB Eliminative Cleavage of the N–N′-Bond Rather Than Reduction, *Org. Lett.*, **2009**, *11*, 5646–5648.

42 E. M. Simmons and J. F. Hartwig, On the Interpretation of Deuterium Kinetic Isotope Effects in C–H Bond Functionalizations by Transition-Metal Complexes, *Angew. Chem., Int. Ed.*, **2012**, *51*, 3066–3072.

43 D. Hirose, M. Gazvoda, J. Košmrlj and T. Taniguchi, Advances and Mechanistic Insight on the Catalytic Mitsunobu Reaction Using Recyclable Azo Reagents, *Chem. Sci.*, **2016**, *7*, 5148–5159.

44 A. Pautard-Cooper and S. A. Evans Jr., Mechanistic Implications of 1,3,2-λ^5-Dioxaphospholanes in the Mitsunobu Reaction, *J. Org. Chem.*, **1989**, *54*, 2485–2488.

45 The readily available known phosphonium cations shown below afforded the amination product **2a** in only low yields (2–7%). See Supporting Information for details.

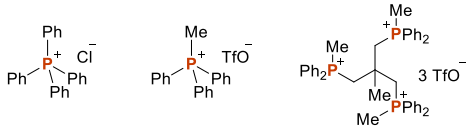

46 T. Lu and Q. Chen, Independent Gradient Model Based on Hirshfeld Partition: A New Method for Visual Study of Interactions in Chemical Systems, *J. Comput. Chem.*, **2022**, *43*, 539–555.

47 T. Lu and F. Chen, Multiwfn: A Multifunctional Wavefunction Analyzer, *J. Comput. Chem.*, **2012**, *33*, 580–592.